MEASUREMENT OF EMI SHIELDING PERFORMANCE OF GRAPHENE OXIDE AND ELECTROCHEMICALLY EXFOLIATED GRAPHENE THIN FILMS

Andjela Stefanović[1,2], Dejan Kepic[1], Miroslav Huskić[3], Kamel Haddadi[4], Mohamed Sebbache[4], Svetlana Jovanović Vučetić[1], Biljana Todorović Marković[1]

[1]*Vinča Institute of Nuclear Sciences - National Institute of the Republic of Serbia, University of Belgrade, P.O.B. 522, 11001 Belgrade, Serbia*
[2]*Faculty of Chemistry, University of Belgrade, Studentski trg 12-16, 11158 Belgrade*
[3]*Faculty of Polymer Technology, Ozare 19, 2380 Slovenj Gradec, Slovenia*
[4]*University of Lille, CNRS, Centrale Lille, University Polytechnique Hauts-de-France, UMR 8520-IEMN, F-59000 Lille, France*
e-mail: andjela.stefanovic@vin.bg.ac.rs

Abstract
Graphene and its derivatives have become the scientific community's focus due to their remarkable electronic, mechanical, and optical properties. In this work, we prepared two graphene-based materials, graphene oxide (GO) and electrochemically exfoliated graphene (EEG), and performed morphological and structural analysis. Both materials showed good dispersibility in water. GO is composed of mainly single- and few-layer graphene sheets, while EEG is predominately multi-layer graphene. EEG showed better thermal stability under nitrogen flow compared to GO. We also performed ElectroMagnetic Interference (EMI) shielding performance measurements of these materials.

Introduction
Electromagnetic pollution is becoming a major worry for us due to the exponential growth of wireless electronics and communication tools [1].
Electronic devices such as laptops and mobile phones emit electromagnetic radiation (EMR), which is a natural byproduct of contemporary technology [2]. The specific absorption rate, or quantity of incoming electromagnetic radiation absorbed over a broad frequency band, determines how these various radiation types influence living things. Beginning with larger wavelengths of non-ionized low-energy radiation like radio waves and microwaves, this spectrum moves through infrared and visible light before ending with shorter wavelengths of higher-energy radiation like ultraviolet, X-rays, and gamma rays [3].
Numerous studies have connected EMR to a number of health hazards, even though the effects of EMR on human health are not yet completely understood, such as DNA damage, cellular stress, lower sperm count and even cancer.
The risks connected with exposure to EMR from electronic devices are particularly of concern, as these devices are typically localized near the body, such as laptops put in laps and mobile phones kept in trouser pockets. Laptops are built up with Radio Frequency electronic devices operating in the frequency range 0.3 - 2.4 GHz whereas mobile phones use RF frequency signals between 0.01 and 4 GHz [2]. Conductive polymer composites (CPCs)-based EMI shielding materials have several advantages over traditional metal-based EMI materials, including being lightweight, low density, inexpensive, easily fabricated, and having good corrosion resistance [1].
Reducing phone usage and utilizing airplane mode when feasible are some ways to safeguard against EMR from computers and mobile phones. Other methods include employing shielding covers or pouches for laptops and phones. It is crucial to remember that even while these methods might lessen exposure to EMR, the danger may still exist. Existing EMR-blocking

textiles have the drawback of potentially blocking helpful signals like cellular and Wi-Fi. In addition, the efficiency of these fabrics can depend on the frequency and intensity of the radiation, as well as the specific fabric and its construction [2].
To produce CPCs-based EMI materials, numerous conductive fillers, including carbon black (CB), carbon nanotubes (CNTs), graphene, carbon nitrides, and metal nanoparticles/nanowires, were used to mixture with insulated polymer matrix [1].

Experimental

GO and electrochemically exfoliated graphene (EEG) were prepared as described previously [4] [5]. Briefly, GO was obtained by modified Hummers' method by oxidation of graphite powder (Sigma-Aldrich) with concentrated sulfuric acid, sodium nitrate and potassium permanganate under elevated temperature (98 °C). After the completion of the reaction, the mixture was diluted, added 2 ml of 30% hydrogen peroxide and the powder was purified by several cycles of centrifugation and washing until reaching neutral pH. EEG was prepared in a two-electrode system using highly oriented pyrolytic graphite rods as both the counter and the working electrode and 0.1 M ammonium persulfate as electrolyte. A direct current (DC) voltage of +12 V was applied, and the voltage was kept constant until the exfoliation process was finished which was indicated by the total consumption of the working electrode. The obtained material was purified by several cycles of centrifugation after which the material was dispersed in water using an ultrasonic bath.
Transmission electron microscopy (TEM) analyses were performed on the TEM-JEOL JEM-1400 microscope operated at an accelerating voltage of 120 kV. The samples were dispersed in ethanol using an ultrasound bath and a drop of dispersion was deposited on lacey carbon copper grids (200 mesh) and dried in air. Raman spectra were recorded on a DXR Raman microscope (Thermo Scientific). Each spectrum was obtained at room temperature using a 532 nm excitation line with a power of 2 mW. The spectral resolution was 1 cm-1 and the acquisition time was 10 × 10 s. The confocal pinhole diameter was 50 µm. Each sample was recorded at four different places and an average spectra was used. Thermogravimetric analysis (TGA) tests were performed on a TGA/DSC 3+ (Mettler Toledo instruments, Greifensee, Schweiz) under nitrogen (20 ml/min) at a heating rate of 5 °C/min, from 25 to 1000 °C. Samples were prepared by passing 15 ml of 1 mg/ml water dispersions through 0.2 µm PC Membrane using a vacuum.EMI shielding efficiency measurements were conducted using a Vector Network Analyzer (VNA) from Keysight Technologies (Streamline P5008A) operating in the frequency range 150 kHz-53 GHz. The VNA is connected through high stable coaxial cables to a dedicated coaxial set-up to measure the complex reflection (S11) and transmission (S21) up to 18 GHz. Preliminary to the microwave characterization of the samples, a vector calibration is performed at the output of the coaxial cables to remove systematic errors. Input RF power was set to -15 dBm, intermediate frequency (IF) bandwidth was set to 100 Hz resulting in a time per frequency of 10 ms. All measurements were conducted at room temperature. Each sample is sandwiched between two thin films of cellulose (named PAPER in the following) to avoid any contamination of the coaxial apertures.

Results and discussion

In this work, we used two types of graphene material: one obtained from graphitic powder by following the modified Hummers' method and one obtained from highly oriented pyrolytic graphite rod by electrochemical exfoliation. Both materials, namely graphene oxide (GO) and electrochemically exfoliated graphene (EEG) are well dispersible in water and form stable dispersions. While the water dispersion of EEG is black in color, the dispersion of GO is brownish which might be an indication of a higher oxidation degree of GO compared to EEG.

To investigate the structural properties of both materials we performed TEM analysis (figure 1). GO sample has a higher degree of single-layer and few-layer graphene than EEG which indicates better exfoliation of GO. Graphene sheets have lateral sizes of up to several hundreds of nanometers and graphene sheets are planar with some wrinkles and folds at the sheet ends. Contrary to GO, the TEM images of EEG reveal the presence of predominately few- and multi-layer graphene with larger sheet dimensions, usually up to several micrometers. Based on the Z-contrast of TEM images a stacking of graphene sheets is notable.

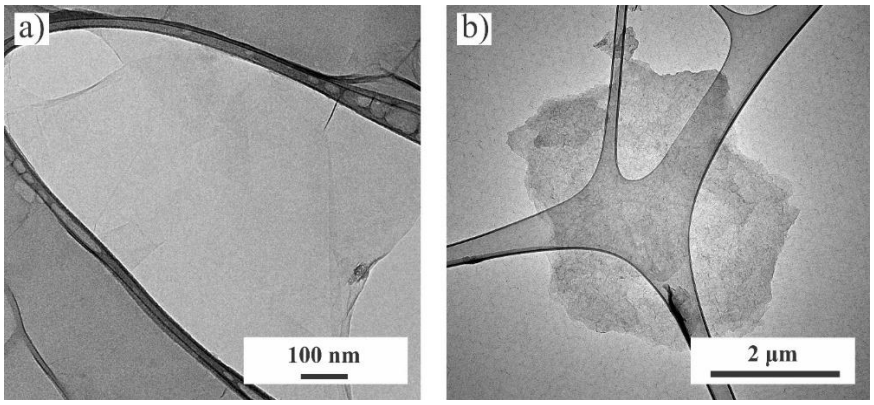

Figure 1. TEM images of a) GO and b) EEG.

Raman spectra of GO and EEG (figure 2) reveal typical graphitic features at 1350 cm^{-1} and 1593 cm^{-1} [6]. The first peak at 1593 cm^{-1} is also known as the G band and originates from the double-degenerate vibrational mode (E_{2g}). It is a first-order scattering process at the crossing of the longitudinal optical (LO) and transverse optical (TO) phonon branches at the Γ point in the first Brillouin zone of graphene. The other peak at 1350 cm^{-1}, denoted as the D peak, is a defect-induced band. It is activated by symmetry breaking induced by the presence of defects or the edges of graphene. Besides, the spectra also show bands that appear at 2700 cm^{-1} and 2930 cm^{-1} that correspond to 2D and D+G bands. The intensity ratio between D and G peaks, also known as I_D/I_G ratio, is an important characteristic of the graphene structures which is related to the defect density and the crystallite size. The I_D/I_G ratio for GO is 0.9, while the I_D/I_G ratio for EEG is 1.2.

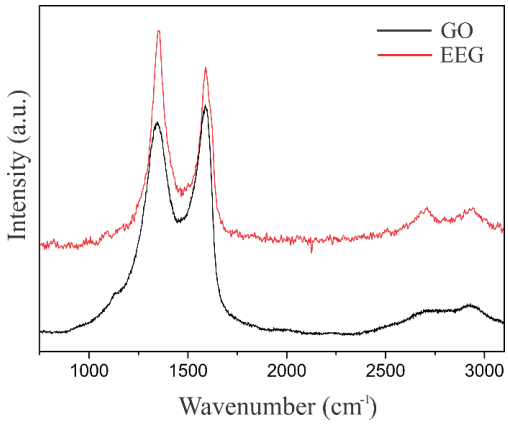

Figure 2. Raman spectra of GO and EEG.

The difference in GO and EEG structure is well reflected in their thermal stability. We performed TGA analysis of both materials under nitrogen and TGA curves are presented in figure 3. The first mass loss region is associated with the loss of adsorbed moisture, the second

mass loss around 200 °C is attributed to the breakdown of thermally labile oxygen-containing functional groups, and the third region to the decomposition of the carbon lattice. TGA curves reveal a significant portion of oxygen functional groups in GO compared to EEG. Additionally, EEG shows better carbon lattice stability - at 1000 °C the residual mass of EEG is 55.14% while GO is 2.8%.

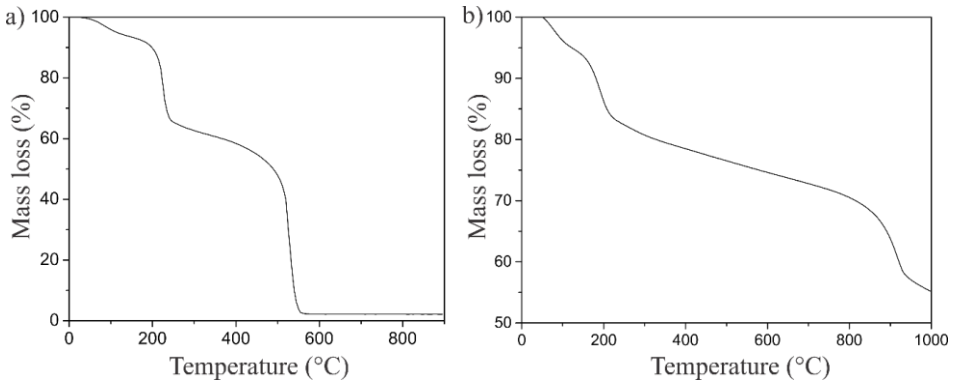

Figure 3. TGA curves of a) GO and b) EEG.

The EMI shielding performance of GO and EEG was estimated by measuring the amplitude of the S-parameters. The data are reported in figure 4. From Fig. b), transmission coefficient of the GO sample does not show any difference with the reference signal (PAPER only), indicating a poor EMI efficiency. Fig. 4 (c) and (d) EEG sample show clear difference between reference and loaded measurements. At 2 GHz, the difference of amplitude of the transmission coefficient S21 is around 10 dB corresponding to 10% of the RF power reflected transmitted through the sample.

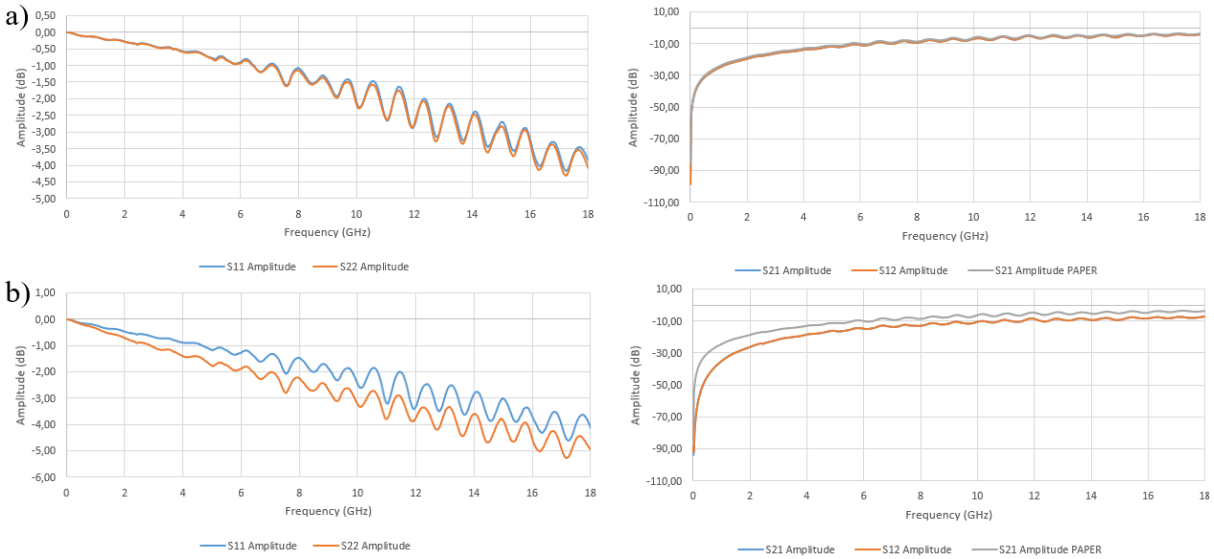

Figure 4. Electromagnetic shielding effectiveness of a) GO and b) EEG in vertical plane.

Conclusion

In this work, we used two types of graphene-based materials – graphene oxide obtained by modified Hummers' method and exfoliated graphene obtained by electrochemical exfoliation. Both materials are well dispersible in water and form a stable dispersions. GO is mainly composed of single- and few-layer graphene sheets, while EEG is predominately multi-layer graphene. Both GO and EEG showed typical features of graphene in the Raman spectra, while I_D/I_G ratio is higher for EEG compared to GO. EEG also showed better thermal stability. EMI shielding performance measurement revealed relatively good performance of the EEG material whereas GO material does not show EM shielding.

Acknowledgements

This project has received funding from the European Union's Horizon Europe Coordination and Support Actions programme under grant agreement No 101079151 - GrInShield. The research was also supported by the Science Fund of the Republic of Serbia, #7741955, Are photoactive nanoparticles salvation for global inflectional treath? - PHOTOGUN4MICROBES and by the Ministry of Education, Science and Technological Development of the Republic of Serbia, grant number 451-03-47/2023-01/200017.

References

[1] Y. Luo, Y. Guo, C. Wei, J. Chen, G. Zhao, Q. Yuan, Y. Zhu, Carbon. 215 (2023) 118480.
[2] U. Ahmed, T. Hussain, H.S. Ahmad, Intern. Jour. of Therm. Sci. 194 (2023) 108594.
[3] S. Ayesha, Z. Abideen, G. Haider, F. Zulfiqar, A. El-Keblawy, A. Rasheed, K.H.M. Siddique, M. B. Khan, E. Radicetti, Plant Stress, 9 (2023) 100198.
[4] Z. Marković, M. Budimir, D. Kepić, I. Holclajtner-Antunović, M. Marinović-Cincović, M. Dramićanin, V. Spasojević, D. Peruško, Z. Špitalský, M. Mičušik, V. Pavlović, B. T. Marković, RSC advances, 6 (2016) 39275-39283.
[5] D. Kepić, S. Sandoval, Á. P. Del Pino, E. György, L. Cabana, B. Ballesteros, G. Tobias Kepić, Chem. Phys. Chem, 18 (2017) 935-941.
[6] L.M. Malard, M.A. Pimenta, G. Dresselhaus, M.S. Dresselhaus, Physics reports, 473 (2009). 473 51-87.